NEW CONCEPT FOR CFRP BASED CONFORMAL LOAD-BEARING ANTENNA STRUCTURE

Ill-Kyung Park, Korea Aerospace Research Institute, Daejeon, South Korea
Sang-Eui Lee, In-ha University, Incheon, South Korea
Woo-Sung Chung, Danam Systems, Anyang, South Korea
Jae-Won Yang, Danam Systems, Anyang, South Korea

Abstract

Conformal Load-bearing Antennas Structure (CLAS) has become widespread to overcome the drawbacks of conventional protruding antennas, such as high aerodynamic drag, increased radar cross section, and structural complexity. Most of CLAS have adopt an external side skin fabricated with dielectric materials to transmit electromagnetic (EM) waves for radio frequency (RF) communication. However, dielectric materials such as glass and quartz fiber possess inferior structural properties, making them unsuitable as primary structural materials. In this study, A novel concept for Carbon composite-based CLAS (CCLAS) has been proposed to enhance structural load-bearing capability. CCLAS has been realized based on four core technologies: the EM window made of GFRP at the center of an external side skin with carbon composite, the lattice core using 3D printing techniques, the Conformal Structural Shield (CSS), and the beamwidth-enhanced EM radiator. A structural and an antenna performance have been verified through the ground and flight test in this study.

1. NOTATION

Acronyms:

CLAS	Conformal Load-bearing Antenna Structure
CCLAS	Carbon composite-based CLAS
EM	Electromagnetic
OML	Outer Mold Line
CSS	Conformal Structural Shield
APTP	Antenna Performance Test Prototype
RSSI	Received Signal Strength Indicator

2. INTRODUCTION

The research and development programs related to CLAS commenced in the early 1990s under the management of the United States Air Force Research Laboratory (AFRL), with two initial projects (Smart Skin Structures Technology Demonstrator (S3TP), RF Multifunction Structure Aperture (MUSTRAP)). Since then, continuous research and development on CLAS have been conducted in US, leading to their eventual commercialization and application on the F-35 fighter jet. (Ref. 1) Noteworthy CLAS-related research in Europe includes the ACASIAS (Advanced Concepts for Aero-Structures with Integrated Antennas and Sensors) Program, initiated in 2017 under the leadership of NLR, focusing on integrating various communication antennas within aircraft fuselage and winglet structures. (Ref. 2) In South Korea, with the aim of application in military aircraft, has conducted CLAS research by the Agency for Defense Development (ADD) and is currently advancing its application to stealth unmanned aerial vehicles based on conceptual and validation studies in Ref. 3. In many previous CLAS studies, it was common to apply an external side skin made of dielectric materials such as a E-glass or quartz fiber composite for EM wave transmission. However, in order to apply CLAS to metallic or carbon composite aircraft structures, skin cut-out or recessed shape had to be incorporated into the airframe. Consequently, such CLAS systems result in the aircraft having increased structural weight and

Copyright Statement

The authors confirm that they, and/or their company or organization, hold copyright on all of the original material included in this paper. The authors also confirm that they have obtained permission, from the copyright holder of any third-party material included in this paper, to publish it as part of their paper. The authors confirm that they give permission, or have obtained permission from the copyright holder of this paper, for the publication and distribution of this paper as part of the ERF proceedings or as individual offprints from the proceedings and for inclusion in a freely accessible web-based repository.

reduced structural integrity, as well as lower load-bearing capacity.

This study aimed to develop a carbon composite-based CLAS that enhances structural load-bearing performance and can be applied as an integrated with carbon composite principal structures. The antenna frequency integrated with the structure was set to the C-band range of 5.03 to 5.15 GHz, which is widely used for unmanned aerial vehicle communication frequencies. Four core technologies were developed to integrate the antenna within the carbon composite structure. To validate both structural and communication performance, prototypes for ground and flight test were fabricated, and test & evaluations were carried out to verify the performance of CCLAS.

3. CCLAS

3.1. Requirements

The requirements for CCLAS established in the study to enhance structural load bearing performance and efficiency of aircraft system are described in Table 1. The requirements for CCLAS were established across three domains: system, structure, and antenna. The requirements in the system are derived from the objectives of R&D program. The structural requirements were considered to be at a level applicable to the lower skin of a medium-sized utility helicopter, while the antenna requirements aimed to achieve performance similar to that of a protruding omni antenna.

3.2. Overview

Figure 1 illustrates the components and core technologies of CCLAS. CCLAS features a sandwich structure, with the upper and lower facesheets made of carbon composite material. The upper facesheet includes an EM window at the center to allow EM wave transmission. A lattice core, manufactured using a 3D printing technique, is employed to position the patch-type EM radiator at the center. A feeding connector is located at the center of the lower facesheet. The core technologies of CCLAS aim to place the antenna within the carbon composite facesheet and ensure stable communication performance and high structural reliability. The four core technologies are:

I. Designing a ply-overlap joint for E-glass fiber EM window within carbon fiber composite facesheet.
II. Designing and manufacturing a 3D-printed lattice core to enhance antenna and structural performance.
III. Implementing a CSS to ensure and stabilize antenna communication performance.
IV. Using a flexible coupled feed connector to improve the durability of the connector.

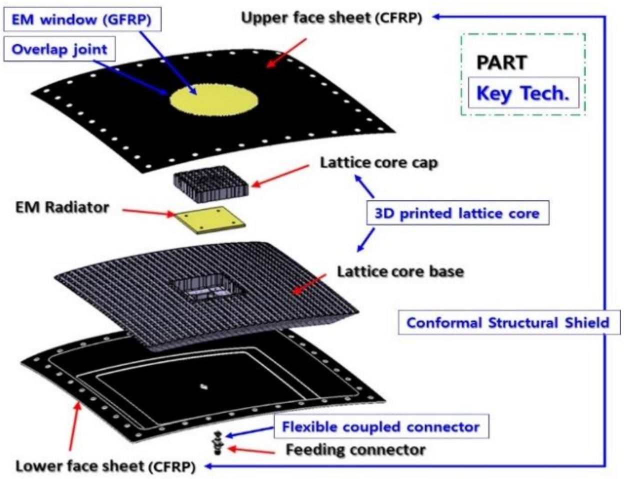

Figure 1: Components and key technologies for CCLAS

4. CORE TECHNOLOGIES

4.1. Ply-overlap joint for EM window

Table 1. Requirements for CFRP based CLAS.

Item		Value	Remark
System	Weight Reduction	> 10 %	vs. protruding antenna
	Part Reduction	> 50 %	
Structure	Compressive Strength	> 833 N/cm	300mmX300m (> 25 kN)
	Impact Resistance	> 5.36 J	ASTM D7136
Antenna	Freq. Range	5.03 ~ 5.15 GHz	C-band
	Return Loss	< -10 dB	S-parameter
	Elevation Angle	0 to 90 deg	
	Azimuth Angle	0 to 360 deg	

A design study was conducted on dissimilar composite ply-overlap joints for applying an EM window made of E-glass composite to the external facesheet of a carbon composite. The aim of this work is to develop a joint design to achieve structural strength, manufacturability, and geometrical tolerance for fabrication. Three types of joints were generated and validated the design through the static and fatigue coupon tests. Figure 2 illustrates the three joint candidates: a staggered joint presented in Ref. 4, a flush joint where the plies of the two materials are simply overlapped, and a hybrid joint that appropriately combines the other joint types. The hybrid joint design was selected as the CCLAS EM window joint design, because it provides not only adequate static and fatigue strengths of joint, but also quite good geometrical tolerance, as shown in the cut cross-section on the right side of Figure 2 (a). The ply-overlap length was selected as 15 mm.

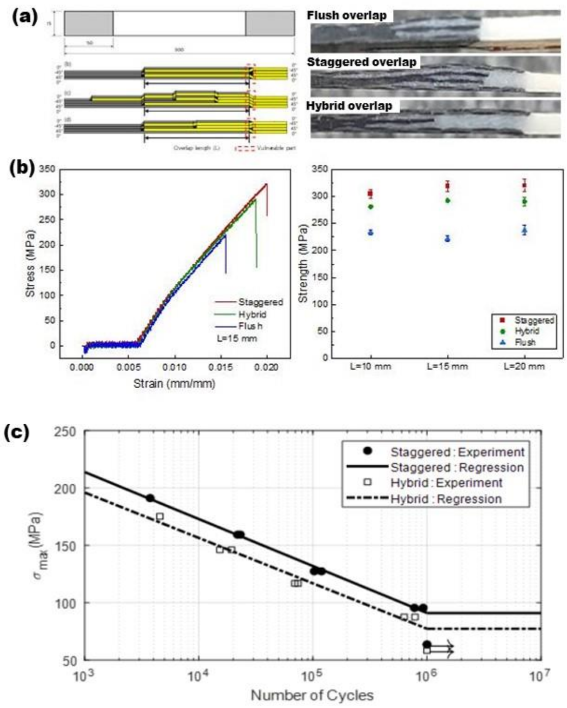

Figure 2: Candiate over-lap joints (a) and static (b) and fatigue (c) properties of each joints

4.2. 3D printed lattice core

Ref. 3 discusses the sandwich panel-type CLAS that has configuration where a patch antenna is placed between the external facesheet and the honeycomb core. This arrangement has the disadvantage of weakening the structural load-bearing performance and potentially damaging the antenna when the external skin is impacted.

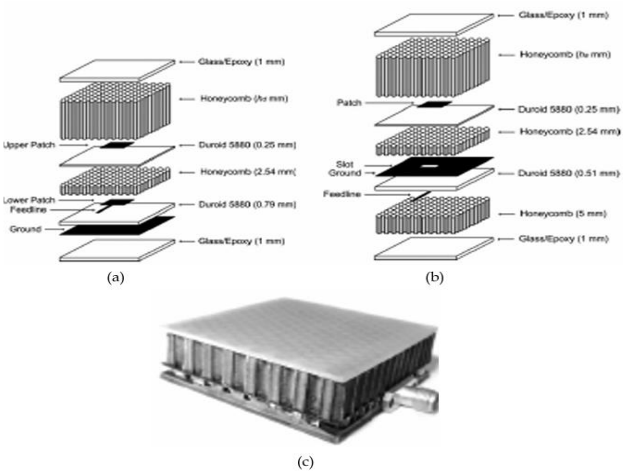

Figure 3: CLAS concept from Ref. 5. (a) Direct-fed stacked patch antenna, (b) aperture-coupled patch antenna, and (c) photograph of a fabricated direct-fed stacked patch antenna.

To address this issue, You et. al (Ref. 5) have also been conducted on a CLAS configuration that places a patch antenna at the center of a double sandwich panel, as shown in Figure 3. However, the design of placing a patch antenna between the core and facesheet has inherent disadvantages that undermine structural integrity and communication stability.

To overcome those and enhance the stability of antenna performance, this study developed a novel 3D-printed lattice core. As shown in Figure 4, the lattice core is composed of a core base and a core cap. It is designed to position the patch antenna at the center of the sandwich panel without any fastening components such as screws. Additionally, the joint between the two core sections incorporates a deliberate segmentation design to prevent excessive stress concentration under structural load, thereby ensuring structural safety and communication stability. A lattice core is based on the compressive strength of an Aramid honeycomb with a cell size of 4.8 mm and a density of 72 kg/m^3, comprising vertical members and diagonal members to enhance shear stiffness and strength characteristics in Ref. 6. The interface design shape, where the facesheet is bonded with an adhesive film, features a segmented square flange structure to minimize crack propagation due to local adhesive damage from impacts. The material for the lattice core is a polymer with excellent high-temperature stability and atmospheric exposure characteristics. Figure 5 depicts the cutting-section of the CCLAS, and interface between the facesheets and the lattice core, which are bonded like hidden line.

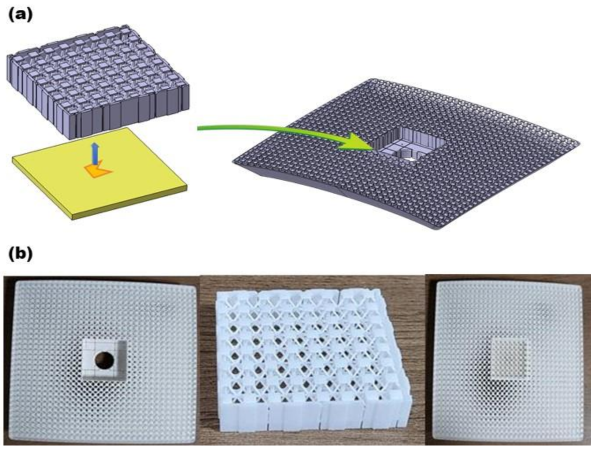

Figure 4: 3D printed lattice core components. (a) Assembly of core base and core cap with EM radiator and (b) printed lattice core components

Figure 5: Cutting-secntion of the CCLAS with 3D printed lattice core

4.3. CSS

In patch antennas embedded within carbon composite panels, EM waves generated by EM radiator can be reflected off the conductive carbon composite facesheet surface, then reflected waves can lead to a degradation in antenna performance. The T-300 grade carbon fabric composite material used in the CCLAS facesheet, which are conductive and woven into a pattern. As described in Ref. 7, the surface roughness caused by the woven pattern leads to scattered reflection waves. These irregular reflected waves significantly affect the EMI-sensitive areas of the patch antenna, such as the feeding connector, resulting in modulation of the return loss (antenna resonance frequency) and changes in the beam pattern.

To enhance communication performance by suppressing the reflected waves originating from the woven fabric carbon composite facesheet, this study developed a Conformal Structural Shield (CSS) by integrating an EM absorber into the inner surface of the facesheet. Figure 6 illustrates the process by which the application of an EM absorber to the conductive surface minimizes the EM reflection by undergoing reflection and absorption processes. When an EM absorber with excellent absorption performance is applied, most of the EM wave attenuation occurs during the initial transmission (1st absorbing) through the EM absorber and after reflection off the conductive plate during the subsequent transmission (2nd absorbing) through the EM absorber.

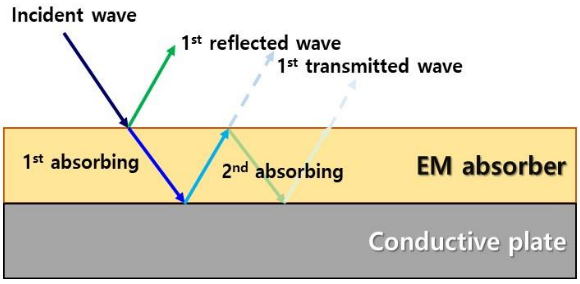

Figure 6: Process of attanuation of EM wave through EM absorber onto conductive plate

In this study, as shown in Figure 7, the CSS was fabricated by integrating the magnetic polymer composite EM absorbing layer into the internal layers of the carbon composite facesheet through a co-curing process. Figure 8 shows the changes in the frequency range and return loss before and after the application of the CSS. Before applying the CSS, the system fails to meet the required frequency range specified in Table 1 and exhibits low return loss values. In contrast, after applying the CSS, not only is the required frequency range met, but the return loss also shows significantly improved results.

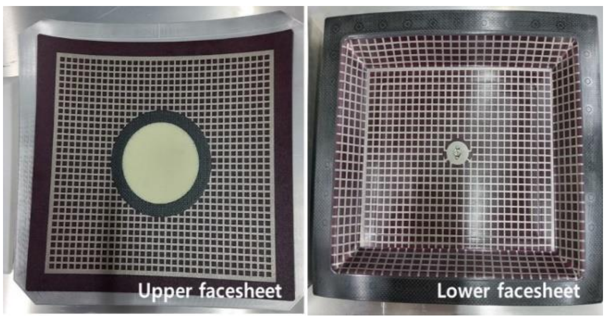

Figure 7: CSS of CCLAS prototype for ground test

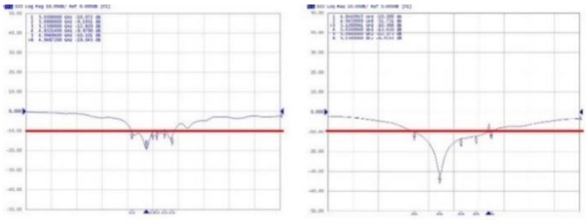

Freq. Range [MHz]	Resonance Freq.	
	Freq. [MHz]	Return Loss [dB]
134 (4,832 ~ 4,996)	4,948	-19.04

(a)

Freq. Range [MHz]	Resonance Freq.	
	Freq. [MHz]	Return Loss [dB]
293 (4,845 ~ 5,138)	4,945	-31.75

(b)

Figure 8: Antenna freq. bandwidth and return loss. (a) without CSS, and (b) with CSS

4.4. Flexible coupled feed connector

The feed device of a patch antenna is typically connected directly to the antenna plate using bolts or soldering. However, when the patch antenna for a CLAS is positioned at the center of a sandwich panel, a connector must be attached to the lower facesheet, and an additional device is required to provide a feed to the patch antenna. Ref. 2 describes the process of addressing the damage to the antenna feed device connector that occurred during structural testing of a CLAS. Connectors and other electrical joints for communication and avionics equipment typically do not consider structural loads and deformations in their design. However, the CCLAS must be developed to ensure stable communication performance even under high structural loads.

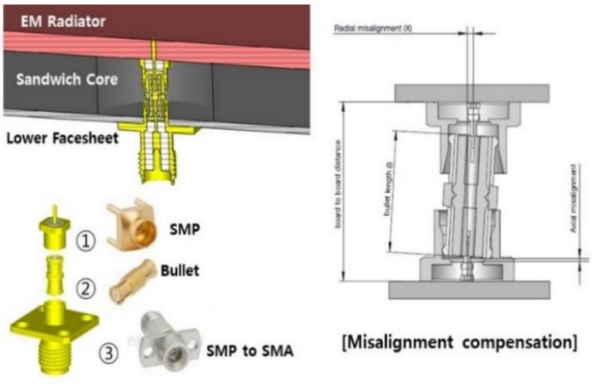

Figure 9: Flexible coupled feed connector to enhance durability of CCLAS

To enhance the durability of the antenna feed device, this study applied a flexible coupled feed connector, as shown in Figure 9. This design includes a swiveling adaptor at the feed point, allowing it to maintain stable feeding capabilities even under significant structural deformation and in high-vibration environments.

4.5. Enhanced antenna beamwidth

With the application of embedded antennas, CLAS typically exhibits the characteristics of a directional antenna with a narrower beamwidth compared to protruding antennas. However, a narrow beamwidth can impair communication performance at various elevation angles.

Therefore, although not a core technology unique to the development of CCLAS, this study developed a patch antenna pattern aimed at broadening the beamwidth to enhance communication strength across various altitude. Figure 10 presents the results of the beamwidth improvement design, achieving up to a 66% increase in beamwidth in different directions.

Item	Basic Rectangular Patch	Developed Patch
Shape		
Freq.	C-band (5.03~5.15 GHz)	←
VSWR	2:1	←
Gain	7.75 dBi	4.5 dBi
Beamwidth	81° / 72° (directional)	130° / 120° (directional)
Beam Pattern	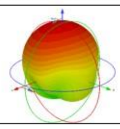	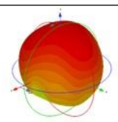

Figure 10: Enhanced antenna beamwidth for CCLAS

5. DESIGN AND VERIFICATION PROCEDURE

5.1. Ground test prototype

The structural load-bearing and antenna performance of the CCLAS were validated through ground and flight testing. Each test aimed at specific purposes and was tailored to fit the aircraft configurations.

The ground test prototype was developed to verify mainly structural performance, focusing on high structural load-bearing capacity, impact resistance, and environmental performance. This prototype was designed to meet the structural requirements outlined in Table 1, capable of supporting the loads applicable to the lower forward fuselage of a medium-sized rotary-wing aircraft. The design incorporated varying cross-sectional curvatures of the fuselage. To generate the main design parameters for the ground test prototype, developmental testing was conducted using an APTP. Figure 11 illustrates the components reflecting the key design features applied to the APTP. Through over 50 design variable trade-off studies, the main design variables for the ground prototype were determined and subsequently used as main reference material for developing antenna performance analysis model and scheme. Figure 12 shows the components and the fabricated ground test prototype of CCLAS with four plies carbon fabric composite facesheet as basic lay-up pattern.

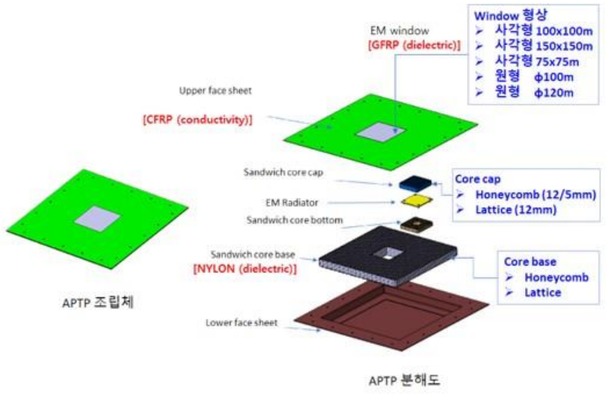

Figure 11: APTP to determine main design variable for CCLAS ground test prototype

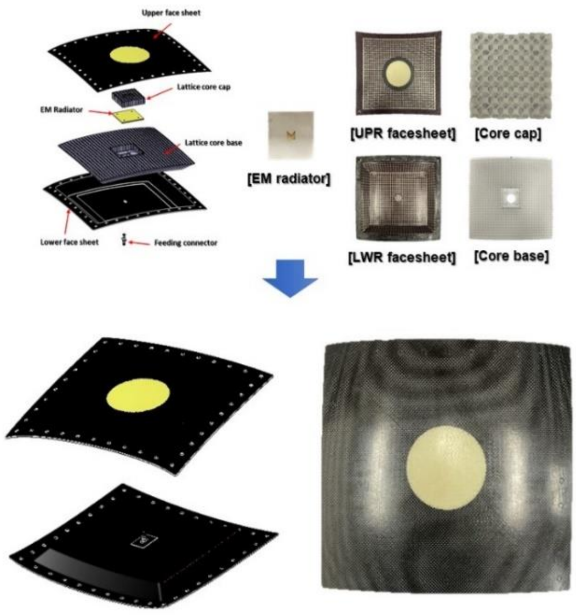

Figure 12: 3D CAD model and fabricated ground test prototype of CCLAS

Figure 13 illustrates the antenna performance test results of the ground test prototype, including Return Loss (S-parameter) and beam pattern configuration. The measured frequency range meets the C-band target of 5.03 to 5.15 GHz specified in this study. The 3D beam pattern demonstrates a uniformly distributed antenna communication performance, and the cross-sectional beam patterns in each direction indicate that no significant nulls occur.

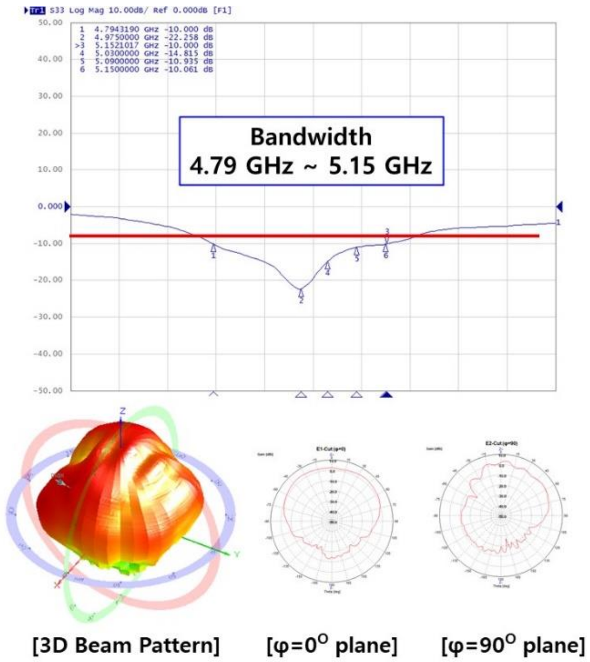

Figure 13: Frequency range and beam pattern results of ground test prototype of CCLAS

5.2. Flight test prototype

The CCLAS flight test prototype was developed to be integrated on the front rear side of tail boom structure of the MPUH (Multi-Purpose Unmanned Helicopter) which is a helicopter with a maximum takeoff weight of 200 kg, as shown in Figure 14. The MPUH is a high-performance unmanned helicopter featuring a carbon composite airframe and a rigid hub with 2-blades. It has a payload capacity of 60 kg, a maximum cruising speed of 150 km/h, and an over 6 hours maximum operating time. The flight test prototype aimed to verify stable communication performance not only in various flight attitudes of a rotary-wing aircraft, but also in the high level of vibration of rotary-wing aircraft and EMI of avionics around it.

Figure 13: Frequency range and beam pattern results of ground prototype of CCLAS

In the MPUH, the C-band RF antenna utilizes a Dipole omni-antenna, with one positioned at the front and another at the rear. These antennas are equipped with an algorithm that automatically switches between them based on signal strength, ensuring optimal communication with ground control antennas. In the flight test prototype studied here, the rear antenna is tasked with communication and is strategically mounted at the bottom of the tail boom. This placement is chosen to enhance communication stability at broad elevation angles.

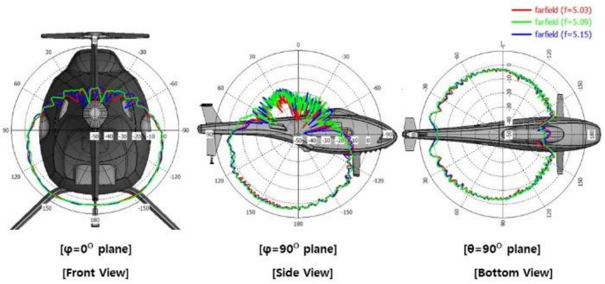

Freq.	Gain [dBi]			HP(3dB) Beamwidth	
	MAX.	$\varphi = 0°$ Elevation Plane	$\varphi = 90°$ Elevation Plane	$\varphi = 0°$ Elevation Plane	$\varphi = 90°$ Elevation Plane
5.03 GHz	+5.86	+4.64	+4.30	126.0°	13.8°
5.09 GHz	+6.38	+5.35	+4.49	120.1°	76.0°
5.15 GHz	+6.95	+5.33	+4.97	117.2°	60.9°

Figure 14: Antenna performance analysis result to position CCLAS at best communication capability

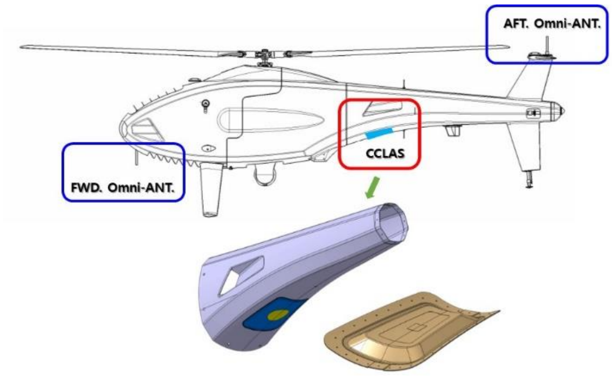

Figure 15: Existing protruding C-band omni-antennas and CCLAS flight test prototype

By employing an antenna performance analysis technique that builds on the previous APTP test results, we determined the optimal location of CCLAS flight test prototype for the lower side of the tail boom of the MPUH, as illustrated in Figure 14. Figure 15 shows both the mounting position of the CCLAS flight test prototype on the MPUH and the installation of the existing protruding C-band antennas. To integrate the CCLAS flight test prototype into the MPUH, a modified finite element analysis (FEA) model was developed by incorporating the CCLAS into the existing airframe structural analysis model. A structural integrity assessment was performed using this model. Figure 16 depicts the fabricated CCLAS flight test prototype, which features a greater curvature compared to the ground test prototype and has a rectangular projection shape with its longitudinal dimension exceeding its width.

Figure 16: Composition and fabricated flight test prototype of CCLAS

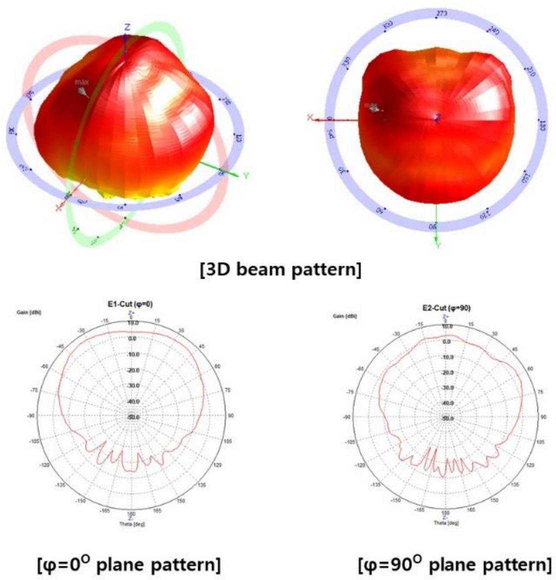

Figure 17: Beam pattern results of flight test prototype of CCLAS

5.3. Ground test

Figure 18 provides a schematic representation of the ground and flight test procedures to verify performance of CCLAS. The ground test is composed of three categories which are structural load-bearing performance tests, antenna performance tests under structural load, and environmental tests.

The first category includes maximum tensile/compression tests, impact load tests, maximum tensile/compression tests after impact tests, and structural fracture tests. Except for the structural fracture test, antenna performance measurements were conducted before and after each structural test to measure any changes in antenna performance. The energy level of impact test was established considering the thickness of facesheet in accordance with ASTM D7136, and total 10 impact loading were implied on the external skin of CCLAS.

The antenna performance tests under structural loading were conducted using a test fixture capable of applying compressive loads on the test specimen within an antenna performance test chamber. This method measured antenna performance stability under structural load, with a maximum compressive load of 15 kN applied due to the operational limitations of the test fixture.

The environmental tests were conducted following the MIL-STD-810H standard and included operational temperature, humidity, and vibration tests. The operational temperature and vibration conditions were established considering the installation on the MPUH unmanned helicopter. As with the other tests, antenna performance tests were also conducted before and after the environmental tests to measure any changes in antenna performance.

5.4. Flight test

The verification of CCLAS flight performance involved comparing the antenna signal strength of the protruding C-band antenna mounted on the rear top of the MPUH, as depicted in Figure 15, with that of the CCLAS flight test prototype under identical flight conditions. To achieve this, the rear fuselage of the MPUH was outfitted with the CCLAS flight test prototype and a protruding Di-pole antenna, as shown in Figure 19. This configuration was combined with an aircraft that had been validated for reliability through over 30 hours of flight, and the combined setup was employed for the flight tests. The testbed aircraft equipped with the CCLAS flight test prototype was designated as MPUH-C. The MPUH-C was engineered to allow for the selection between the rear protruding antenna and the CCLAS via a switch mechanism. To mitigate the risk of aircraft failure due to CCLAS malfunction during flight tests, the tests were conducted with a protruding antenna installed on the front fuselage.

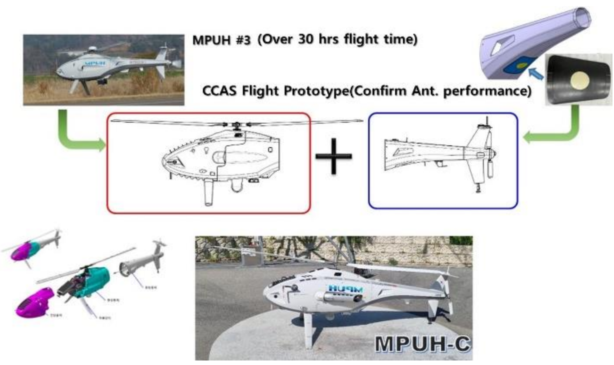

Figure 19: MPUH-C intagrated both the CCLAS and the Di-pole antenna mounted on the tail boom

As illustrated in Figure 18, the CCLAS flight test is divided into CCLAS integration tests and antenna performance flight tests. The CCLAS integration test involves measuring the antenna communication

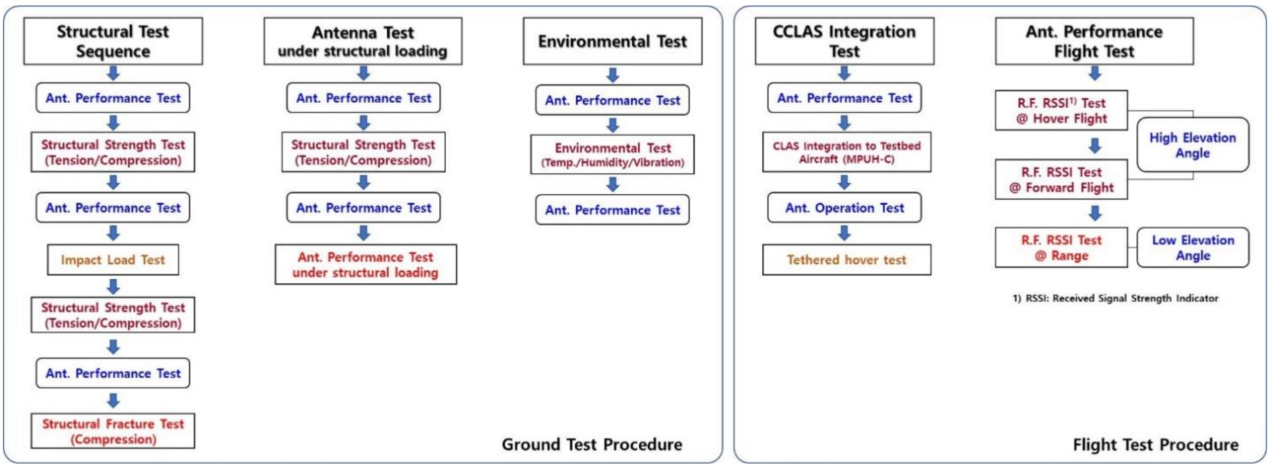

Figure 18: Ground and flight test procedures for verification of CCLAS

performance before and after integration, followed by a tethered flight test to assess the normal flight capability and communication status of the MPUH-C.

The antenna performance flight test is categorized into high elevation performance tests and low elevation performance tests. The high elevation performance tests involve measuring RSSI while gradually increasing altitude in a hovering state, thereby validating communication performance with changes in elevation angle. The low elevation performance tests measure RSSI in relation to changes in aircraft forward flight speed, distance from the GCS (Ground Control System) antenna, and variations in the aircraft's nose direction.

6. RESULTS AND DISCUSSION

6.1. Ground test results

As the first step of the structural load-bearing performance test, a 25 kN compressive load structural test was carried out, and the structural integrity was confirmed. The antenna frequency range measured before and after the test satisfied the C-band condition, and there was almost no change in the beam pattern. Figure 20 shows the test execution configuration and the results of the communication performance measurement before and after the test.

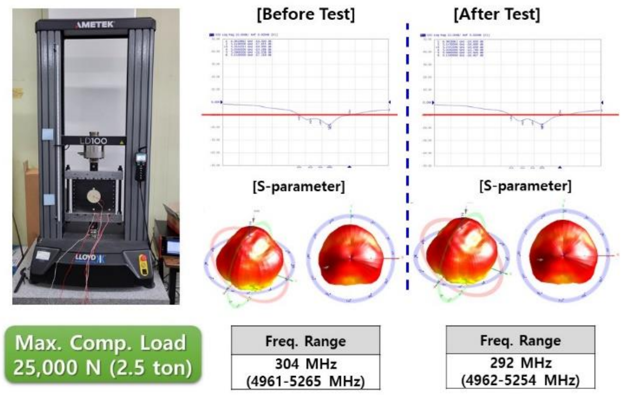

Figure 20: Antenna performance measurements before and after structural load-bearing performance test

Figure 21 presents the antenna performance measurement results for the test specimen before and after the impact test. The frequency range increased by approximately 30% after the test, but still met the C-band frequency requirements. The beam pattern showed no significant changes before and after the test. The results of the tensile/compression test conducted after the impact test also confirmed that structural integrity was maintained.

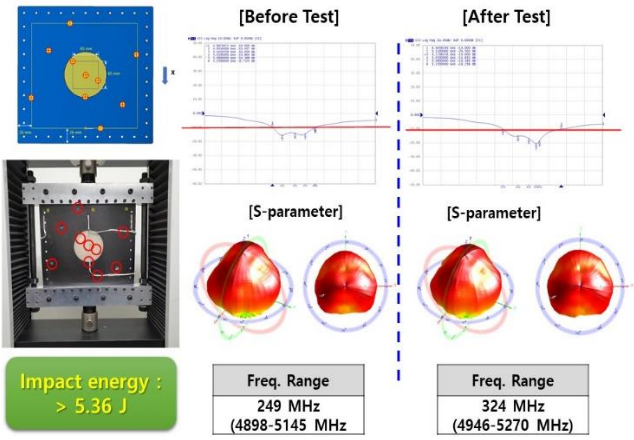

Figure 21: Antenna performance measurements before and after impact load test

As the final step of the structural load-bearing performance test, a compression fracture test was conducted. A compressive load was applied to the test specimen, which had sustained partial damage to the outer skin from the impact test, until failure occurred. Failure was observed at a compressive load of approximately 57.9 kN. The failure initiated with buckling of the side members of the CCLAS and progressed to the failure of the adhesive bonding area between the upper and lower facesheets. Figure 22 shows the force-stroke curve of the compression failure test, depicts that the load increased linearly before the failure occurred.

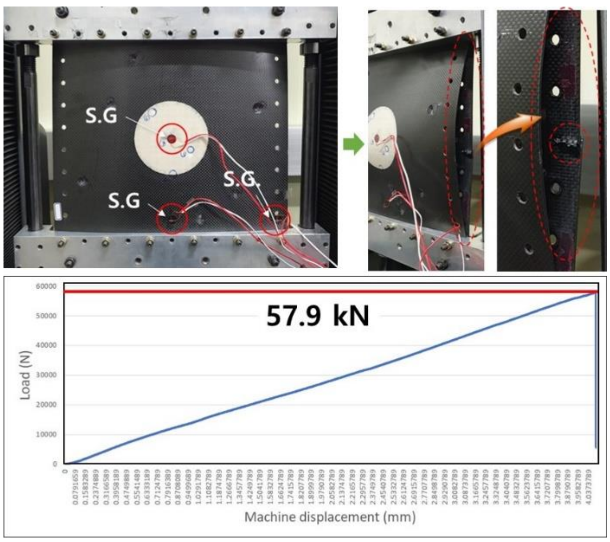

Figure 22: Structural fracture test (compression) results of CCLAS ground test specimen

To evaluate the stability of antenna performance under structural loading, the frequency range and beam pattern were measured while gradually increasing the load up to 15 kN within the antenna performance test chamber, and the results were compared. As shown in Figure 23, there was minimal change in the frequency range and beam pattern even under a structural load of 15 kN.

No	Test case	Freq.	Gain [dBi]			HPBW (3dB)		
		Bandwidth (S11 ≤ -10dB)	5.03 GHz	5.09 GHz	5.15 GHz	5.03 GHz	5.09 GHz	5.15 GHz
(1)	GT #5 (EM Radiator, 0 N)	303 MHz (4962-5265 MHz)	4.34	3.94	3.39	115.3°	114.3°	107.7°
(2)	GT #5 (EM Radiator, 2000 N)	-	3.90	3.53	2.81	113.6°	114.3°	105.0°
(3)	GT #5 (EM Radiator, 5000 N)	-	4.13	3.73	3.15	114.6°	115.4°	108.0°
(4)	GT #5 (EM Radiator, 10000 N)	-	4.15	3.80	3.24	115.8°	114.3°	103.7°
(5)	GT #5 (EM Radiator, 15000 N)	306 MHz (4962-5268 MHz)	3.98	3.54	3.05	116.8°	117.6°	109.1°

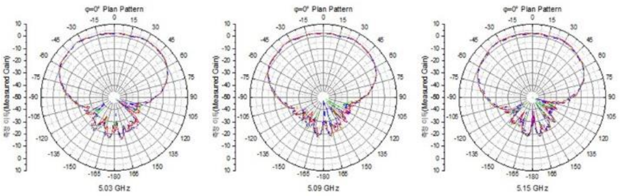

Figure 22: Antenna performance stablity under structural loading

Figure 23 presents the results of the antenna performance measurements taken before and after the environmental tests, indicating that there was minimal change in antenna performance following the tests.

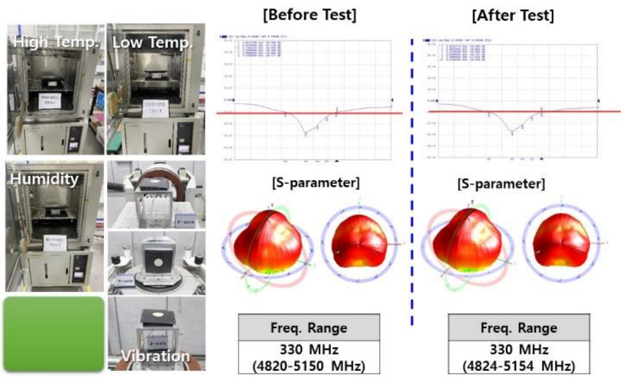

Figure 23: Antenna performance measurements before and after environment tests

6.2. Flight test results

After assembling the MPUH-C system, it was secured to a ground test fixture, and the communication transmission and reception capabilities were verified using the CCLAS flight test prototype. Commands were forced to key components such as the engine and rotor, and the status information of the aircraft was received by GCS, confirming the proper functioning of both the uplink and downlink. As depicted in Figure 24, a tethered test setup was used to evaluate normal aircraft operations, including engine startup, hovering, and low-speed turning flights.

Figure 24: Communication & quasi-flight test of MPUH-C with tethered test setup

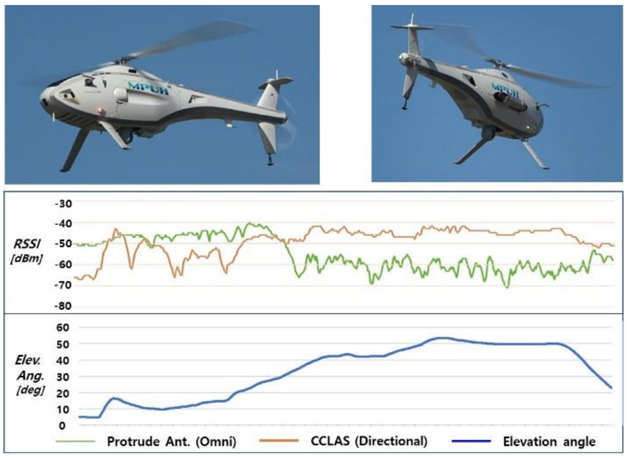

Figure 25: RSSI results with respect to elevation angle during hovering flight test

Figure 25 shows the results of measuring RSSI while gradually increasing the elevation angle through changes in altitude during hovering. Flight tests were carried out using both the existing protruding antenna and the CCLAS, and the results were compared. Reliable communication is achievable when RSSI is above -70 dBm. The hovering altitude was increased to 20 m, 50 m, and 100 m, and RSSI was checked from a minimum elevation angle of 5 degrees up to 55 degrees. The existing protruding antenna, characteristic of an omni-antenna, exhibited high signal strength at lower elevation angles but gradually weakened as the elevation angle increased, sometimes dropping below -70 dBm beyond the maximum angle. In contrast, the CCLAS showed some fluctuation at lower elevation angles but maintained RSSI above -70 dBm, and demonstrated stable and strong reception strength at elevation angles above 20 degrees.

Second type of flight test was forward flight along with race track. During the second flight test, RSSI was compared with and without the option to automatically switch between the front and rear antennas of the MPUH-C based on signal strength, while the aircraft performed a flight along a race track at a constant altitude and speed around the GCS antenna. Even with the CCLAS applied, the automatic switching of the front and rear antennas based on signal strength operated effectively.

When not using automatic antenna switching, RSSI of the CCLAS was higher than that of the protruding antenna, depending on the elevation angle and the position of the GCS antenna. When automatic switching was enabled, both antenna configurations showed similar signal strengths. Additionally, with automatic switching, RSSI of the CCLAS appeared relatively stable.

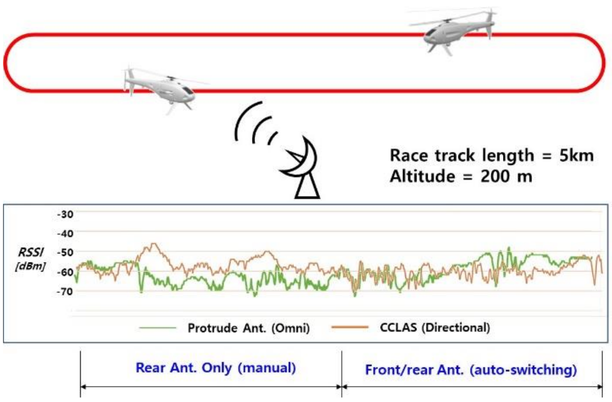

Figure 26: RSSI results based on aircraft heading and antenna auto-switching application

6.3. Discussion

Through the ground testing of the CCLAS, it was confirmed that it exhibits both high structural load-bearing performance and maintains structural integrity and communication performance even under external impacts loading. The application of the 3D printed lattice core made stable communication performance despite damage to the facesheet surface from multiple impact loads. Additionally, the CCLAS displayed excellent damage tolerance characteristics, with failure occurring at loads exceedingly twice the maximum operational load. This stable communication performance was also verified during antenna performance tests under structural load. Environmental testing according to MIL-STD-810H confirmed that the CCLAS operates effectively in practical aviation environments. Overall, the ground test results indicate that the CCLAS provides high damage tolerance and stable performance under significant vibrations, confirming its effective applicability to rotary-wing aircraft.

The flight tests of the CCLAS validated its stable and excellent communication performance. The system maintained consistent signal strength from low to high elevation angles, and the directional antenna characteristics provided superior performance at higher angles. Additionally, antenna performance verification during forward flight confirmed that the CCLAS could be used in conjunction with existing protruding antennas.

Figure 27 compares the beam pattern measurement results of a reference prototype equipped with a blade-type C-band antenna mounted on the same carbon composite sandwich panel structure as the CCLAS, with those of the CCLAS ground test prototype. Due to the reflective characteristics of carbon composite materials, the stable beam pattern of a standalone antenna becomes distorted, resulting in multiple nulls. In contrast, the CCLAS exhibited a relatively stable beam pattern. This phenomenon explains why, during the second flight test, the signal strength of the CCLAS was found to be more stable compared to the protruding antenna.

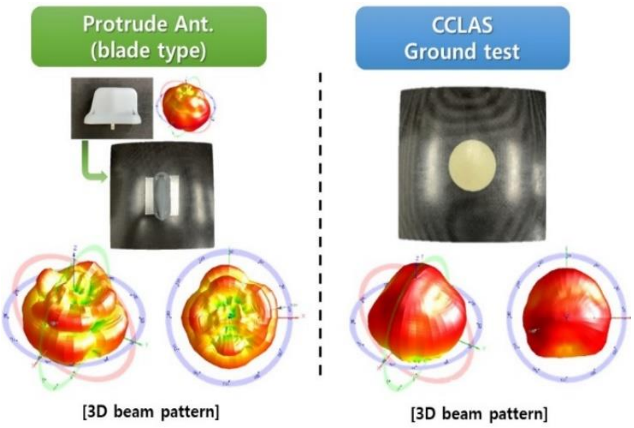

Figure 27: Comparison of 3D beam patterns between the reference blade antenna installation structure and the CCLAS ground prototype

The comparison blade-type antenna and its installation structure in Figure 27 were used as a comparative reference for meeting the system requirements of weight and component reduction, as outlined in Table 1. The CCLAS ground test prototype achieved a 24% of weight reduction and a 71% of part reduction compared to the reference model.

7. CONCLUSIONS

This research aimed to develop a CCLAS that not only enhances structural load-bearing performance but also enables seamless integration with carbon composite airframe structures. Furthermore, the study focused on developing a CCLAS with superior impact resistance and vibration performance tailored for rotary-wing aircraft structures. The outcomes of this research can be summarized as follows:

1. Identified and developed four key technologies necessary for the development of CCLAS, and verified their effectiveness through ground and flight tests.
2. Developed an APTP for the creation of a ground test prototype of CCLAS, from which optimal design variables were derived.
3. Established ground test items and procedures to verify the structural performance of CCLAS, and conducted validation research to confirm system performance suitable for rotary-wing aircraft.
4. Applied a MPUH as the test aircraft for CCLAS flight performance verification. A CCLAS flight test prototype was created and applied to this aircraft.
5. Developed flight test items and procedures to verify the antenna communication performance and applicability of the CCLAS to the aircraft, and conducted validation research accordingly.
6. Through comparative tests and evaluations with a protruding antenna structure, superior structural and antenna performance was confirmed. The objectives of weight reduction and reduction in the number of components were also achieved.
7. CCLAS is expected to have high utility as a communication device for the MUM-T system, demonstrating stable communication performance across various flight attitudes, along with structural excellence.

Author contact:

ILL-KYUNG PARK mechguy77@kari.re.kr

8. ACKNOWLEDGMENTS

This research was supported by Unmanned Vehicles Core Technology Research and Development Program through the National Research Foundation of Korea (NRF) and Unmanned Vehicle Advanced Research Center (UVARC) funded by the Ministry of Science and ICT, the republic of Korea (2020M3C1C1A01084216).

9. REFERENCES

1. Callus P. J., "Conformal Load-Bearing Antenna Structure for Australian Defence Force Aircraft", DSTO-TR-1963, *Defence Science and Technology Organisation*, 2007.
2. Verpoorte, J., "Requirements and Specification Document - WP1", *ACASIAS*, Ref. Ares(2017) 4852899, Sep. 2017.
3. Kim, M. S., Park, C. Y., Cho, C. M. and Jun S. M., “Ground Test & Evaluation of Conformal Load-bearing Antenna Structure for Communication and Navigation”, *J. of The Korean Society for Aeronautical and Space Science*, Vol. 41(11), 2013, pp. 891-899. DOI:http://dx.doi.org/10.5139/JKSAS.2013.41.11.891
4. Ahamed, J., Joosten, M., Callus, P., Wisnom, M. R., and Wang, C. H., “Ply-overlap Hybrid Technique for Joining Dissimilar Composite Materials,” *Material & Design*, Vol. 100, 15 June, 2016, pp. 157-167.
5. You, C.S., Hwang, W., Park, H.C., Lee, R.M., and Park, W.S., “Microstrip Antenna for SAR Application with Composite Sandwich Construction: Surface-Antenna-Structure demonstration,” Journal of Composite Materials, Vol. 37, (4), 2003, pp. 351-364.
6. HexWeb® HRH-10 Aramid Fibre/Phenolic Honeycomb, HEXCEL, Product Data Sheet
7. Xiao, H., Shi, M., and Chen, J., “Electromagnetic Function Textiles,” *Electromagnetic Materials and Devices*, 2019, pp. 1-30. DOI:http://dx.doi.org/10.5772/intechopen.85586

10. CLASSIFICATION & COPYRIGHT

The paper must be unclassified for release to the public and cleared by the appropriate company and/or

government agency if necessary. CEAS and its national member societies shall be allowed to publish the paper. The copyright information is stated on the Forum website https://www.rotorcraft-forum.eu/ and on the front page of this template. All papers presented at the ERF will be published as ERF proceedings. In addition they will be available in a freely accessible web-based repository 2 years after the respective conference.